quantum beam science

MDPI

Article

Proton-Cluster-Beam Lethality and Mutagenicity in *Bacillus subtilis* Spores

Yoshihiro Hase [1,2,*], Katsuya Satoh [1,2], Atsuya Chiba [1], Yoshimi Hirano [1], Kengo Moribayashi [2] and Kazumasa Narumi [1]

[1] Takasaki Advanced Radiation Research Institute, National Institutes for Quantum and Radiological Science and Technology (QST), 1233 Watanuki, Gunma, Takasaki 370-1292, Japan; sato.katsuya@qst.go.jp (K.S.); chiba.atsuya@qst.go.jp (A.C.); hirano.yoshimi@qst.go.jp (Y.H.); narumi.kazumasa@qst.go.jp (K.N.)

[2] Institute for Quantum Life Science, National Institutes for Quantum and Radiological Science and Technology (QST), 8-1-7 Umemidai, Kizugawa, Kyoto 619-0215, Japan; moribayashi.kengo@qst.go

* Correspondence: hase.yoshihiro@qst.go.jp; Tel.: +81-27-346-9032

Citation: Hase, Y.; Satoh, K.; Chiba, A.; Hirano, Y.; Moribayashi, K.; Narumi, K. Proton Cluster Beam Lethality and Mutagenicity in *Bacillus subtilis* Spores. *Quantum Beam Sci.* **2021**, *5*, 25. https://doi.org/10.3390/qubs5030025

Academic Editors: Hidetsugu Tsuchida and Klaus-Dieter Liss

Received: 26 April 2021
Accepted: 25 August 2021
Published: 28 August 2021

In order to compare the molecular nature of the mutation between 1 MeV H^+ and 2 MeV H_2^+, the whole genome sequencing analysis was performed. Genomic DNA was isolated from surviving colonies at the fluence giving a surviving fraction between 0.01 to 0.1. The fluence or dose giving a surviving fraction around 0.01 to 0.1 is commonly used for mutagenesis of bacteria, because the surviving fraction in this range has been empirically known to give the highest mutation frequency. Since there was some inter-experimental variability, we chose the fluences giving a surviving fraction between 0.01 to 0.1 in each mutation analysis experiment.

The mutation frequency showed a negative relationship with surviving fraction (Figure S1; R = −0.73). The mutation frequency ranged from 59.3 to 107.8 × 10^{-8} /bp and was 13 to 23 times higher than that of mock-irradiated samples (4.7 × 10^{-8} /bp). Only SBS was detected in mock-irradiated samples, whereas SBS, Insertion, Deletion and SV were detected in the irradiated samples (Table S1). The G:C to A:T, A:T to T:A and G:C to T:A were relatively frequent (18% or more) whereas G:C to C:G were less frequent (8% or less) in all irradiated samples (Figure S2). A total of four SBS (two G:C to T:A, and one each of G:C to A:T and G:C to C:G) were observed in the mock-irradiated sample. Single-base deletion was the most frequent deletion event; the number of deletion events decreased with increasing deletion size (Table S2). The SV accounted for 1.5% to 8.0% of total mutation events (Table S1). We detected 21 SVs in total and, except for one SV, succeeded in predicting their overall structure (Table S3, Figure S3). Of those 20 SVs, seven were simple inversions, and more than half of the SV events involved translocation and/or deletion ≥1 kb. Although the reason is unclear, 1 MeV H^+ tended to induce SVs more than twice as often as 2 MeV H_2^+.

In sum, we could not find a clear difference in the molecular nature of the mutation between 1 MeV H^+ and 2 MeV H_2^+.

Methods

The whole Genome Sequencing was performed using 100 ng of genomic DNA. The genomic DNA was extracted from a 2 mL overnight culture using the Wizard Genomic DNA Purification Kit (Promega, Tokyo, Japan). Sequencing libraries were prepared using a KAPA HyperPlus Kit (Nippon Genetics Co., Ltd., Tokyo, Japan) and IDT for Illumina TruSeq DNA UD Indexes (Illumina K.K., Tokyo, Japan) according to the manufacturer's instructions but with half the reaction volume. Sequencing was performed by the company Novogene (Beijing, China) using the NovaSeq 6000 system (Illumina); 150 bp paired-end reads were generated.

The raw sequencing reads were cleaned using Illumiprocessor (version 2.0.9 [1]), and the cleaned data were mapped to the reference sequence of *B. subtilis* (NC_000964.3 [2])

using BWA (version 0.7.5 [3]), SAMtools (version 1.3.1 [4]), and Picard-tools (version 1.119 [5]). The candidate mutation sites were identified using GATK Haplotype Caller (version 3.4 or 4.1.8 [6]), Pindel (version 0.2.4 [7]), and BreakDancer (version 1.4.5 [8]) algorithms. The average depth of coverage was at least 30 fold, and more than 99.8% of the genome was covered a minimum of 10 times. Candidate mutation sites detected in more than two independent samples were excluded as false positives or background mutations existing in our lab strain. The candidate mutation sites were considered as unique and fixed mutations if allele frequencies (AF; proportion of mutant reads at a site) were higher than 80% and, for all the other samples, if the AFs were lower than 5%. All candidate mutations were confirmed with Integrative Genomics Viewer (IGV, version 2.8.13 [9]). The detected mutations were classified into seven categories (see [10,11]): single-base substitution (SBS), single-base deletion (−1), single-base insertion (+1), deletion of two or more base pairs (Del ≥ 2 bp), insertion of two or more base pairs (Ins ≥ 2 bp), complex type (Complex), and structural variant (SV). The complex category represents more than two SBS, insertion and/or deletions separated by fewer than 10 bp, and they were considered to have resulted from a single mutation event whereas SV represents inversion and translocation, which may involve deletion and/or duplication at the junction sites. The junction points and overall structure of SVs were confirmed with IGV. If two SVs, unconnected via their junction points, were observed in the same sample, they were regarded as independent mutation events. The reliability of our mutation detection method was validated by PCR and Sanger sequencing [10,11].

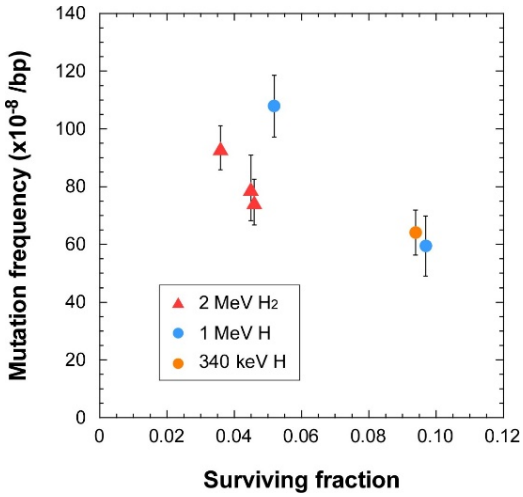

Figure S1. Relationship between surviving fraction and total mutation frequency (the sum of all types of mutations). The data points represent mean ± standard error of survived colonies obtained from experiments listed in Table S1.

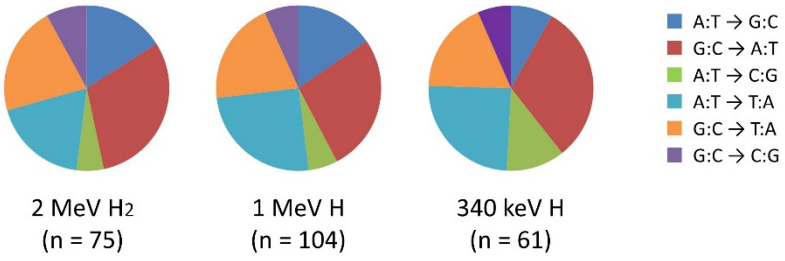

Figure S2. Spectra of single-base substitutions. The data for 2-MeV H_2^+ and 1-MeV H^+ are from Experiment III listed in Table S1.

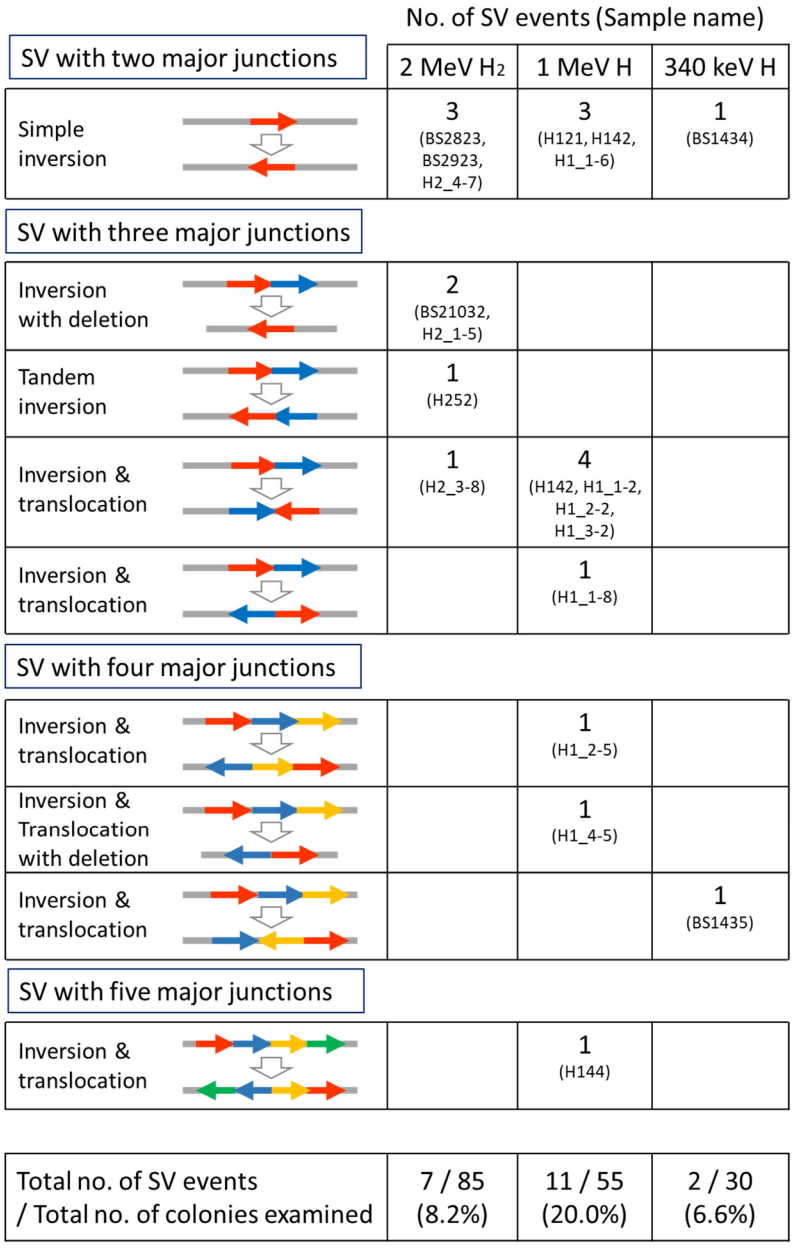

Figure S3. Schematic representation of the predicted overall structure of SVs. The deletions ≥ 1 kb associated with SVs are also given. The SV detected in H1_2-7 are not included because we failed to predict the overall structure.

Table S1. Frequency of each mutation type.

Beam	Exp.	Fluence (p/cm²)	Fluence (atm/cm²)	Dose (Gy)	Surviving Fraction	No. of analyzed colonies	SBS	-1	Del ≥ 2 bp	1	Ins ≥2 bp	Complex	SV	Total
							Mutation frequency (× 10^{-8} / bp) (Percent to total in each experiment)							
2 MeV H_2^+	I	5×10^{10}	1×10^{11}	6032	0.045	20	54.6 ± 8.6 (68.7%)	10.7 ± 3.2 (13.4%)	10.7 ± 3.2 (13.4%)	nd	nd	2.4 ± 1.6 (3.0%)	1.2 ± 1.2 (1.5%)	79.5 ± 11.5
	II	5×10^{10}	1×10^{11}	6032	0.036	30	71.2 ± 7.0 (76.3%)	8.7 ± 2.4 (9.3%)	9.5 ± 2.2 (10.2%)	0.8 ± 0.8 (0.8%)	0.8 ± 0.9 (0.8%)	nd	2.4 ± 1.3 (2.5%)	93.3 ± 7.6
	III	5×10^{10}	1×10^{11}	6032	0.046	35	50.8 ± 6.2 (68.2%)	4.7 ± 1.9 (6.4%)	9.5 ± 2.5 (12.7%)	nd	1.4 ± 0.9 (1.8%)	6.1 ± 2.2 (8.2%)	2.0 ± 1.1 (2.7%)	74.6 ± 7.9
1 MeV H^+	I	5×10^{10}	5×10^{10}	3016	0.097	20	36.8 ± 7.8 (62.0%)	2.4 ± 1.6 (4.0%)	8.3 ± 3.1 (14.0%)	3.6 ± 1.9 (6.0%)	nd	3.6 ± 1.9 (6.0%)	4.7 ± 2.8 (8.0%)	59.3 ± 10.4
	III	1×10^{11}	1×10^{11}	6032	0.052	35	70.5 ± 8.6 (65.8%)	14.9 ± 3.8 (13.9%)	14.2 ± 2.6 (13.3%)	nd	nd	2.7 ± 1.3 (2.5%)	5.4 ± 1.7 (5.1%)	107.8 ± 11.1
340 keV H^+	II	2×10^{10}	2×10^{10}	2400	0.094	30	48.2 ± 6.8 (75.3%)	5.5 ± 1.9 (8.6%)	5.5 ± 1.9 (8.6%)	3.2 ± 1.5 (4.9%)	nd	nd	1.6 ± 1.1 (2.5%)	64.0 ± 7.8
Mock	I	0	0	0	1	20	4.7 ± 2.8 (100.0%)	nd	nd	nd	nd	nd	nd	4.7 ± 2.8

Mutation frequency represents the number of mutation events divided by the length of the reference genome (4,215,606 bp); the values are mean ± standard errors of survived colonies. nd: not detected.

Table S2. Distribution of deletion size.

Deletion size (bp)	2-MeV H_2^+	1-MeV H^+	340-keV H^+
1	27 (44%)	26 (48%)	7 (50%)
2–9	22 (36%)	20 (37%)	4 (29%)
10–99	7 (11%)	4 (7%)	0 (0%)
≥ 100	6 (6%)	4 (7%)	3 (21%)
Total no. of deletions	62	54	14
Total no. of colonies Examined	85	55	30

Data for 1-MeV H^+ and 2-MeV H_2^+ are the sum of two and three independent experiments, respectively, and the data for the 340-keV H^+ is from single experiments listed in Table S1.

Table S3. Predicted SVs.

Beam	Exp.	Sample name	Approx. position of the rejoined sites on the reference genome	Predicted Alteration *
2 MeV H_2^+	I	H252	1,211,380 2,365,590 2,519,790	Tandem inversion
	II	BS21032	391,350 Del (391,350–397,190) 3,082,740	Inversion with 5.8-kb deletion
		BS2823	1,212,290 1,364,960	Simple inversion
		BS2923	3,691,560 3,948,320	Simple inversion
	III	H2_1-5	2,154,090 Del (3,052,800–3,053,830) 3,054,120	Inversion with 1.0-kb deletion
		H2_3-8	608,580 734,720 3,795,680	Inversion & translocation
		H2_4-7	561,550 1,955,970	Simple inversion
1 MeV H^+	I	H121	56,100 4,110,210	Simple inversion
		H142	1,044,880 3,602,660	Simple inversion
			1,199,850 2,162,040 2,990,510	Inversion & translocation
		H144	495,920 2,778,110 2,332,070 2,621,020 3,132,560	Inversion & translocation
	III	H1_1-2	2,374,350 2,374,440 2,374,670	Inversion & translocation
		H1_1-6	1,305,440 3,123,000	Simple inversion
		H1_1-8	964,420 1,153,710 3,429,390	Inversion & translocation

		H1_2-2	1,151,990 3,461,620 Del (3,461,620–3,462,120) Del (3,462,350–3,462,520) 3,462,650	Inversion & translocation
		H1_2-5	428,980 3,708,560 Del (4,118,190–4,121,530) Del (4,121,620–4,122,140) Del (4,122,340–4,122,970) 4,122,970	Inversion & translocation with 3.3-kb deletion
		H1_2-7	575,060 Del (575,060–624,640) 624,640 625,300	Unclear **
		H1_3-2	989,230 3,220,260 3,888,460	Inversion & translocation
		H1_4-5	1,704,680 1,711,610 2,997,950 3,188,050	Inversion & translocation
340 keV H^+	II	BS1434	2,148,200 3,687,940	Simple inversion
		BS1435	301,690 618,510 1,244,420 2,080,110	Inversion & translocation

* Approximate deletion sizes are indicated for those predicted structural alterations involving deletions larger than 1 kb.

** Overall structure is unclear because the sequence reads at least at one of the junction sites, for which the positions are not shown in this table, were mapped to multiple locations on the genome because of the redundancy in the reference sequence.

References

1. Illumiprocessor: Parallel adapter and quality trimming. Available online: https://illumiprocessor.readthedocs.io/en/latest/ (accessed on 12 March 2021).
2. *Bacillus subtilis* subsp. *subtilis* str. 168. Available online: https://www.ncbi.nlm.nih.gov/genome/ (accessed on 12 March 2021).
3. Burrows-Wheeler Aligner. Available online: http://bio-bwa.sourceforge.net/ (accessed on 12 March 2021).
4. SAMtools. Available online: http://samtools.sourceforge.net/ (accessed on 12 March 2021).
5. Picard. Available online: https://broadinstitute.github.io/picard/ (accessed on 12 March 2021).
6. Genome Analysis Toolkit. Available online: https://gatk.broadinstitute.org/hc/en-us (accessed on 12 March 2021).
7. Pindel. Available online: http://gmt.genome.wustl.edu/packages/pindel (accessed on 12 March 2021).
8. BreakDancer. Available online: http://breakdancer.sourceforge.net/ (accessed on 12 March 2021).
9. Integrative Genomics Viewer. Available online: http://software.broadinstitute.org/software/igv/ (accessed on 12 March 2021).
10. Hase, Y.; Satoh, K.; Kitamura, S.; Oono, Y. Physiological status of plant tissue affects the frequency and types of mutations induced by carbon-ion irradiation in Arabidopsis. *Sci. Rep.* **2018**, *8*, 1–10, doi:10.1038/s41598-018-19278-1.
11. Hase, Y.; Satoh, K.; Seito, H.; Oono, Y. Genetic Consequences of Acute/Chronic Gamma and Carbon Ion Irradiation of Arabidopsis thaliana. *Front. Plant. Sci.* **2020**, *11*, 336, doi:10.3389/fpls.2020.00336.